
# Cu-based coatings for IT-SOFC applications

# Cu-Based Coatings for IT-SOFC Applications



ECS Transactions, 91 (1) 2291-2298 (2019)
10.1149/09101.2291ecst ©The Electrochemical Society

# Cu-Based Coatings For IT-SOFC Applications

M. Tomas, C. Goebel, J-E. Svensson and J. Froitzheim

Energy and Materials, Chalmers University of Technology
Kemivägen 10, 41296 Gothenburg, Sweden

Cu and Ce/Cu coated Sanergy HT samples were exposed at 650 °C and 850 °C for 500 h in air + 3 % water vapor and characterized. Mass gain data of all samples were measured throughout exposure. Cr-evaporation measurements were conducted and compared with uncoated Sanergy HT materials. Furthermore, SEM analysis on BIB cross-sections were performed on exposed samples. Results have shown higher mass gain for samples exposed at 850 ºC than 650 ºC as well as higher Cr evaporation. Microstructural analysis shows thinner oxide scales for samples coated with reactive elements.

## Introduction

Solid Oxide Fuel Cells (SOFCs) are a promising technology to face the increasing demand for more sustainable energy. However, many challenges have to be faced (1). One of the most critical one is the corrosion of the metallic interconnects, that occurs during the operating time. To deliver high power output, cells have to be stacked and electrically connected with interconnects. The decrease of the operating temperature below 900 °C allows the use of metallic interconnects, but those suffer from corrosion due the high working temperature. Nowadays, Ferritic Stainless Steel (FSS) is the most widely used class of materials for interconnect applications. The advantages of this material are the low cost compared to previously used ceramics, compatible thermal expansion coefficient properties, high conductivities and ease of production. Custom-made steels such as Crofer 22 APU and Sanergy HT had a considerable success in recent years but were extremely expensive, thus a shift toward large-scale produced steel, such as AISI 441, promises further cost saving (2, 3). Two main mechanisms occur during the operating time: a) the formation of a $Cr_2O_3$ layer which increases the electrical resistance and b) the Cr evaporation from the Cr-rich surface oxide which poisons the cathode. To mitigate the Cr vaporization, coatings are applied on steel surface. $(Mn,Co)_3O_4$ (MCO) coating can be considered as the state-of-the-art coating. Instead of applying MCO directly to the steel, a thin metallic layer (640 nm) of Co can also be applied. This layer will then be oxidized to $Co_2O_3$ and then enriched in Mn by diffusion from the steel substrate, during stack operation (4). The same process can be used to coat samples with Cu. The main advantage of applying a metallic coating instead of ceramic coating, is the price reduction, since the coating can be applied in large scale roll-to-roll process before shaping the interconnect. To further increase the corrosion resistance, a thin layer of reactive element, such as Ce, is added in combination with the metallic coating. It has been shown that even a very thin layer (10 nm) of reactive element can reduce the thickness of the oxide scale significantly (5). The thickness of the oxide scale is a crucial factor mainly for two reasons: a) the depletion of Cr, as the oxide scale forming element and b) the continuously growing $Cr_2O_3$ scale, as a moderate electronic conductor, considerably increases the Area Specific Resistance

(ASR). Research on different copper-based coatings have been conducted by Grolig et al. (6). These have shown that the copper-based coatings investigated do not improve the corrosion resistance at high temperature (around and above 800 °C) and lead to a fast mass gain. The coatings investigated in this work were Ce/Cu and Cu, which have so far not been studied at IT-SOFC conditions and could show promising results such as good Cr retention. The main advantages of copper coatings are a) the reduced prize compared to cobalt coatings and b) the high theoretical electrical conductivity of the copper spinel oxides. *Petric et al.* (7, 8) have shown that copper-based spinels are highly conductive. The highest conductivity was found for $Cu_{1.3}Mn_{1.7}O_4$ with a conductivity of 225 $S \cdot cm^{-1}$ at 750 ºC (8). In these studies, they conclude that the best candidates for interconnects are ferrite spinels, such as $CuFe_2O_4$ and manganite spinels, such as $Mn_xCo_{3-x}O_4$ or $Cu_xMn_{3-x}O_4$.

## Experimental

The composition and characteristics of the materials used in this study, are describe in the following TABLE I and TABLE II.

**TABLE I.** Composition of the studied alloys in weight %, as specified by the manufacturer.

| Materials | Manufacturer | Fe | Cr | C | Mn | Si | Mo | W | Nb | Ti | Add |
|---|---|---|---|---|---|---|---|---|---|---|---|
| Sanergy HT Thickness: 0.02 cm | AB Sandvik Materials Technology | Bal. | 22.4 | 0.01 | 0.25 | 0.07 | 0.93 | <0.01 | 0.41 | 0.06 | Zr |

All samples were coated by AB Sandvik Materials Technology using a Physical Vapor Deposition (PVD) process (9). TABLE II shows what coatings were applied. Before exposure the samples were cleaned in acetone and ethanol using an ultrasonic bath.

**TABLE II.** Characteristics of the materials used. The coating was applied to large sheets of the substrate and the samples were cut out of the steel sheets.

| Materials | Coating | | Geometry | Surface modification | Exposure conditions |
|---|---|---|---|---|---|
| | Inner | Outer | | | |
| Sanergy HT | 10 nm Ce | 600 nm Cu | 15 mm × 15 mm | As-received | 500 h 650 °C and 850 °C Air + 3 % $H_2O$ |
| Sanergy HT | 600 nm Cu | | 15 mm × 15 mm | As-received | 500 h 650 °C and 850 °C Air + 3 % $H_2O$ |

### Cr Evaporation

Cr vaporization in a major issue for the longevity of the fuel cell stack. Therefore, it is necessary to quantify the Cr evaporation during the exposure. The Cr vaporization characteristics of all samples were investigated using the denuder technique which allows in-situ determination of Cr evaporation. The detailed description of the Cr-evaporation

measurement procedure can be found elsewhere (10). All measurements were carried out at 650 °C and 850 °C, in air atmosphere containing 3 % water vapor and a defined air flow of 6000 S·min$^{-1}$ was employed.

Electron Microscopy

Cross-sections of Ce/Cu and Cu coated Sanergy HT samples that were exposed for 500 h were milled using a Leica EM TIC 3X Broad Ion Beam (BIB) with an acceleration voltage of 6.5 kV. The resulting cross-sections were analyzed using Zeiss LEO Ultra 55 FE-SEM.

## Results and Discussion

Mass gain

Figure 1 shows the mass gain behavior of all samples exposed to humid air at 650 °C and 850 °C. At 650 ºC, Ce/Cu-coated samples showed a mass gain lower than that recorded for Cu-coated samples. After 500 h, the mass gain was $1.6\times10^{-1}$ mg·cm$^{-2}$ and $4\times10^{-1}$ mg·cm$^{-2}$ respectively. These results are similar to Ce/Co- and Co-coatings, 0.25 mg·cm$^{-2}$ and 0.3 mg·cm$^{-2}$ respectively, at 650 °C reported by *Falk Windisch and Magrasó* (4, 11). The same trend is observed after 500 h of exposure at 850 °C. The mass gains of Cu-coated samples were around 1.05 mg·cm$^{-2}$ while the mass gains of Ce/Cu coated samples were around 0.88 mg·cm$^{-2}$. These values are in the same range of values of Ce/Co- and Co-coatings (0.7 mg·cm$^{-2}$ and 1 mg·cm$^{-2}$ respectively, at 850 °C) after 500 h exposure (4, 11).

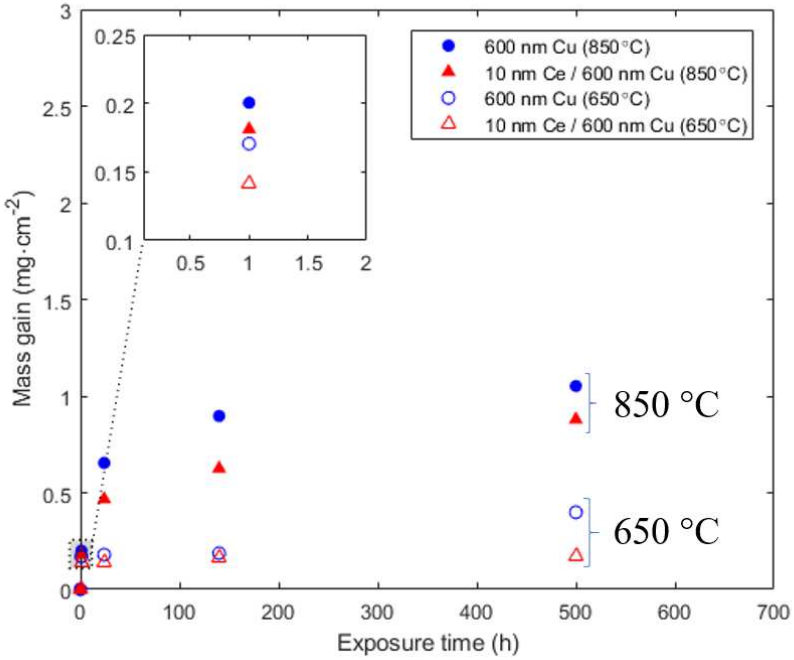


Figure 1. Average mass gain of 600 nm Cu-coating (circles) and 10 nm Ce/600 nm Cu-coating (triangles) for Sanergy HT after 500 h of exposure in air atmosphere containing 3 % $H_2O$. Filled symbols represent the samples exposed at 850 °C and open symbols represent the samples exposed at 650 °C.

Cr evaporation measurements

Cu and Ce/Cu coatings at 650 °C. The data from the Cr vaporization measurements are depicted in Figure 2. Figure 2a shows the Cr evaporation rate and the accumulated Cr vaporization can be found in Figure 2b. Cu-based coatings exhibit a much lower Cr evaporation than the uncoated samples (see Figure 2a). After 500 h, Cu and Ce/Cu coatings mitigate the Cr vaporization by roughly 86 % compared to uncoated materials. Moreover, at 650 °C, Cu-based coatings show a significantly lower Cr evaporation rate than uncoated samples. Ce/Cu- and Cu coatings show a rate of Cr vaporization in the same range than Ce/Co- and Co-coated coatings (approximately $7\times10^{-6}$ mg·cm$^{-2}$·h$^{-1}$) at 650 °C (4).

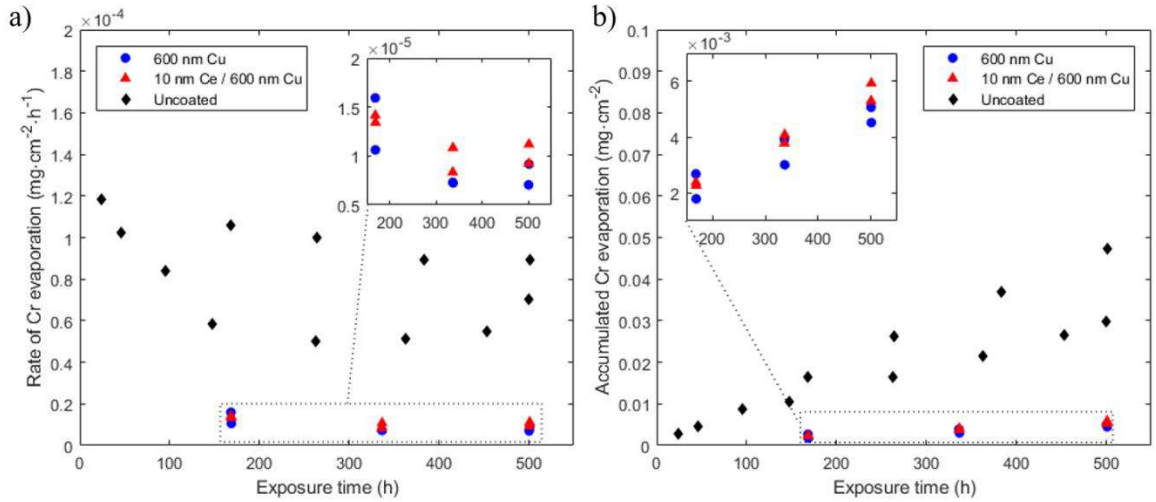


Figure 2. (a) Rate of Cr evaporation as a function of time and (b) Accumulated rate of Cr evaporation as a function of time for Cu-coated Sanergy HT (blue circles), Ce/Cu-coated Sanergy HT (red triangles) and uncoated Sanergy HT (black diamonds) exposed for 500 h at 650 °C in air containing 3 % water vapor. Values for uncoated samples were previously reported by *Falk Windisch et al.* (12) and are depicted for comparison.

Cu and Ce/Cu coatings at 850 °C. The chromium evaporation measurements are shown in Figure 3 and are subject to significant variation. Both Cu and Ce/Cu exhibit a Cr vaporization rate of approximately 0.3 mg·cm$^{-2}$·h$^{-1}$ at 850 °C. The accumulated value for both materials after 500 h is approximately 0.15 mg·cm$^{-2}$. This is about one order of magnitude higher than earlier reported values for Co and Ce/Co coatings ($2.31\times10^{-2}$ mg·cm$^{-2}$ after 500h) (13, 14). In fact, the values for Cu and Ce/Cu seem to be slightly higher than the values reported by *Falk Windisch et al.* (4). This might be due to slight modifications in the measurement technique or could be attributed to an increased Cr transport in Cu spinels as postulated by *Talic et al.* (15).

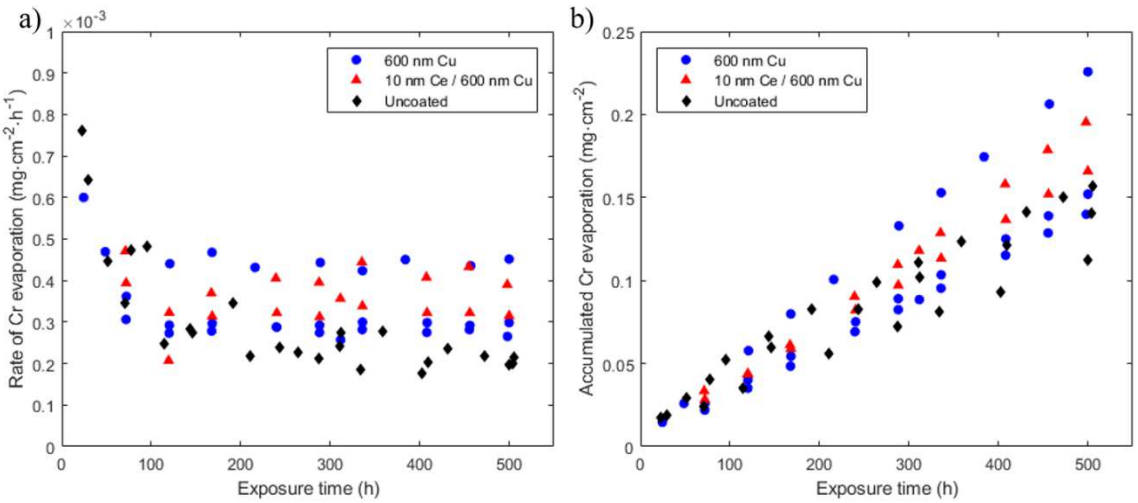


Figure 3. (a) Rate of Cr evaporation as a function of time and (b) Accumulated rate of Cr evaporation as a function of time for Cu-coated Sanergy HT (blue circles), Ce/Cu-coated Sanergy HT (red triangles) and uncoated Sanergy HT (black diamonds) exposed for 500 h at 850 °C in air containing 3 % water vapor. Values for uncoated samples were previously reported by *Falk Windisch et al.* (12) and are depicted for comparison.

Microstructural Analysis

Cu and Ce/Cu coatings at 650 °C. Micrographs of the cross-sections of Cu- and Ce/Cu-coated samples and the corresponding EDX maps are depicted in Figure 4. The Cu coated sample is covered with a CuO top layer with rather high Fe concentration (~ 14.6 cation%) as dopant. The second layer is hematite ($Fe_2O_3$) with a high level of Cr (~ 10.7 cation%) and beneath it, a thick chromia layer is observed. The same layer structure is observed for Ce/Cu-coated samples but is much thinner. The iron oxide layer is highly doped with Cr (~ 30 cation%), Mn (~ 4.2 cation%) and Cu (~ 36.5 cation%). These micrographs show the effect of Ce as a reactive element. It reduces the oxide scales thickness significantly. This effect has been shown by *Falk Windisch et al.* (4, 16). However, Ce/Co coating exposed to the same conditions do not show as much pores as on Ce/Cu coating micrographs (4).

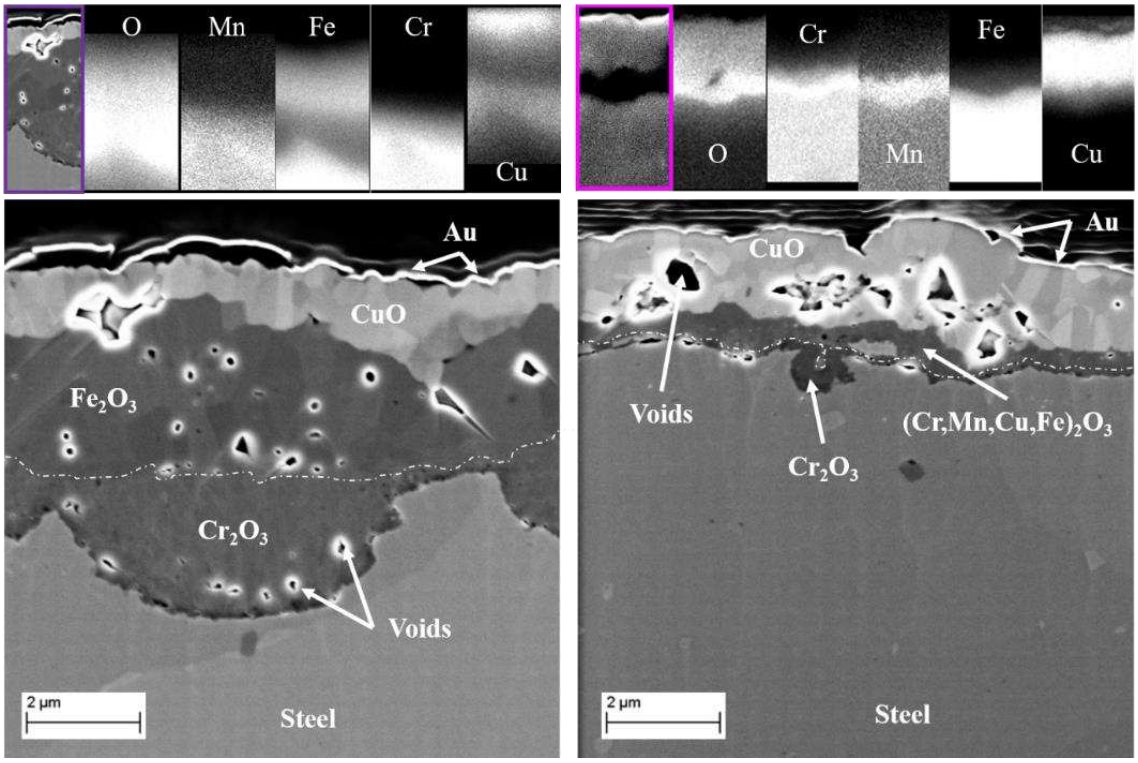


Figure 4. SEM micrographs of BIB milled cross-sections and corresponding EDX map. Left Cu-coated Sanergy HT and right Ce/Cu-coated Sanergy HT. Both exposed 500 h at 650 °C in in air atmosphere containing 3 % water vapor. The dashed line represents the interface between the two oxide layers.

Cu and Ce/Cu coatings at 850 °C. Figure 5 shows the cross-sections of Cu- and Ce/Cu-coated samples and the corresponding EDX maps. The Cu coated sample exhibits an outer spinel layer that consists mainly of Cu (~ 34.2 cation%), Cr (~ 56.5 cation%) and Mn (~ 7.4 cation%), whereas the inner layer consists of a relatively pure chromium oxide (Cr 39 at%, O 60 at% and Fe 1 at%). A similar structure is observed for Ce/Cu coating, but the oxide scales are slightly thinner, which is attributed to the reactive element effect. Cu coating do not improve corrosion resistance at high temperature. This observation is in accordance with previous published work (17, 18), which investigated $(Cu,Mn)_3O_4$ coatings. These publications reported the formation of pores in the oxide scale at temperature above 850 ºC and the substrate suffered from severe corrosion. *Talic et al.* (15) suggests that Cu increases the diffusion rate of Cr in the spinel phase.

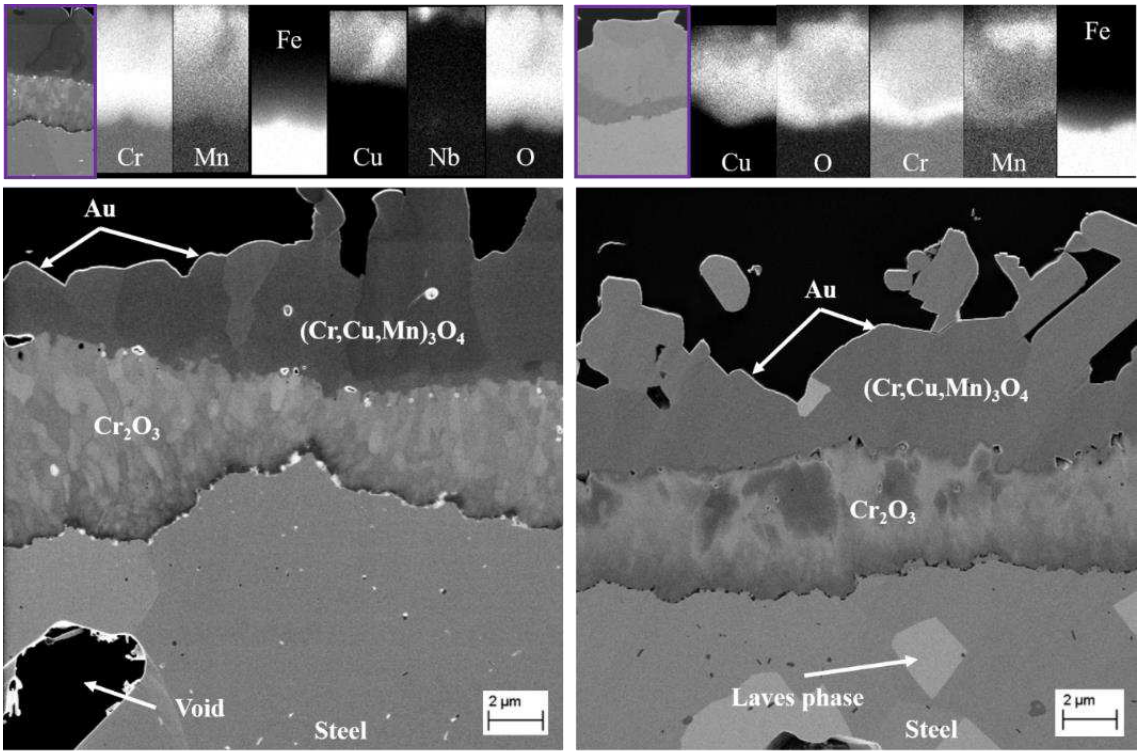


Figure 5. SEM micrographs of BIB milled cross-sections and corresponding EDX map. Left Cu-coated Sanergy HT and right Ce/Cu-coated Sanergy HT. Both exposed 500 h at 850 °C in in air atmosphere containing 3 % water vapor.

## Conclusion

This study shows that at 650 ºC, Cu and Ce/Cu-coatings perform equally good as Co-coatings. Similar mass gains as Co-coatings were measurements for Cu-coatings and gravimetric data shows lower mass gains for Ce/Cu-coated samples. Chromium evaporation data were collected for Cu-coatings and show very similar Cr evaporation values as Co-coatings. The microstructural analysis shows thinner oxide layers for samples coated with Ce than ones coated with Cu only, which correlates well with the observed behavior on Co and Ce/Co coatings.

At 850 ºC, Cu-coatings do not seem to have a positive effect on Cr volatilization. Cr evaporation measurements data show slightly higher Cr vaporization for Cu-coated samples than uncoated materials. Moreover, Cr evaporation is one order of magnitude higher for Cu-coatings compared to Co-coatings. The microstructural analysis showed the presence of a Cr rich spinel phase on top of a thick chromia layer.

These results show that Cu-coatings are not suitable at high temperature (850 ºC) but might be well suited for lower operating temperatures (650 ºC).

## Acknowledgments

The authors are grateful for funding by the Swedish Energy Agency (grant 2015-009652), the FFI program, as well as the Swedish High Temperature Corrosion Centre.

## References


1. Brandon, N., *Solid Oxide Fuel Cell Lifetime and Reliability: Critical Challenges in Fuel Cells*. 2017: Academic Press.
2. Jeffrey W. Fergus, R.H., Xianguo Li, David P. Wilkinson, Jiujun Zhang, *Solid Oxide Fuel Cells: Materials Properties and Performance*. 2009: Taylor & Francis Group LLC.
3. Mahato, N., et al., *Prog. Mater Sci.*, **72**, 141 (2015).
4. Falk-Windisch, H., et al., *J. Power Sources*. **343**, 1 (2017).
5. Polman, E., T. Fransen, and P. Gellings, *J. Phys.: Condens. Matter*. **1**, 4497 (1989).
6. Grolig, J.G., et al., *ECS Trans*. **57**, 2339 (2013).
7. Ling, H. and A. Petric. *Electrical and thermal properties of spinels*. in *207th ECS Meeting* (2005). Quebec City, Canada.
8. Petric, A. and H. Ling, *J Am Ceram Soc*. **90**, 1515 (2007).
9. H. Holmberg, M.W.L., J. Westlinder, *Recent Development in Pre-coating of Stainless Steel Strips for Interconnects at Sandvik Materials Technology*, in *10th European SOFC Forum*. 2012.
10. Froitzheim, J., et al., *J Electrochem Soc*. **157**, B1295 (2010).
11. Magrasó, A., et al., *Int. J. Hydrogen Energy*. **40**, 8579 (2015).
12. Falk-Windisch, H., J.E. Svensson, and J. Froitzheim, *J. Power Sources*. **287**, 25 (2015).
13. Froitzheim, J., et al., *J. Power Sources*. **220**, 217 (2012).
14. Sachitanand, R.N., *Thin-film Coated Steel Foils as Interconnects for Solid Oxide Fuel Cells (SOFC): Oxidation and Chromium Evaporation Properties*. 2015: Chalmers University of Technology.
15. Talic, B., et al., *Solid State Ionics*. **332**, 16 (2019).
16. Alman, D. and P. Jablonski, *Int. J. Hydrogen Energy*. **32**, 3743 (2007).
17. Lv, Y., S. Geng, and Z. Shi, *J. Alloys Compd.*, **726**, 269 (2017).
18. Wei, P., M.R. Bateni, and A. Petric, *J Mater Sci*. **47**, 5205 (2012).